ACS OMEGA

Open Access

http://pubs.acs.org/journal/acsodf

Article

Self-Organized SERS Substrates with Efficient Analyte Enrichment in the Hot Spots

Published as part of ACS Omega virtual special issue "Celebrating 50 Years of Surface Enhanced Spectroscopy".

Volodymyr Dzhagan,* Nazar Mazur, Olga Kapush, Mykola Skoryk, Yaroslav Pirko, Alla Yemets, Vladyslav Dzhahan, Petro Shepeliavyi, Mykhailo Valakh, and Volodymyr Yukhymchuk

Cite This: *ACS Omega* 2024, 9, 4819−4830

Read Online

ACCESS | Metrics & More | Article Recommendations | Supporting Information

ABSTRACT: One of the requirements of an efficient surface-enhanced Raman spectroscopy (SERS) substrate is a developed surface morphology with a high density of "hot spots", nm-scale spacings between plasmonic nanoparticles. Of particular interest are plasmonic architectures that could enable self-localization (enrichment) of the analyte in the hot spots. We report a straightforward method of fabrication of efficient SERS substrates that comply with these requirements. The basis of the substrate is a large-area film of tightly packed SiO_2 spheres formed by their quick self-assembling upon drop casting from the solution. Thermally evaporated thin Ag layer is converted by quick thermal annealing into nanoparticles (NPs) self-assembled in the trenches between the silica spheres, i.e., in the places where the analyte molecules get localized upon deposition from solution and drying. Therefore, the obtained substrate morphology enables an efficient enrichment of the analyte in the hot spots formed by the densely arranged plasmonic NPs. The high efficiency of the developed SERS substrates is demonstrated by the detection of Rhodamine 6G down to 10^{-13} mol/L with an enhancement factor of $\sim 10^8$, as well as the detection of low concentrations of various nonresonant analytes, both small dye molecules and large biomolecules. The developed approach to SERS substrates is very straightforward for implementation and can be further extended to using gold or other plasmonic NPs.

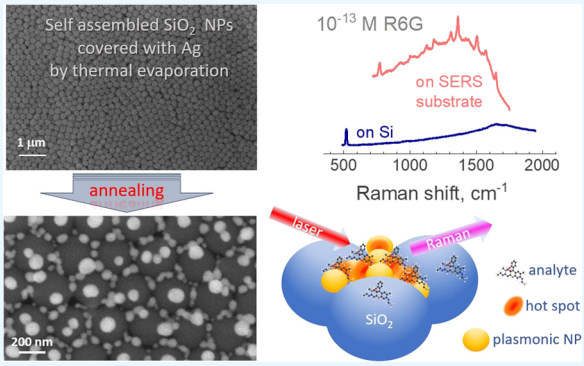

1. INTRODUCTION

Surface-enhanced Raman spectroscopy (SERS) has already demonstrated its great potential for ultrasensitive chemical analysis of both organic[1−9] and inorganic[4,10,11] substances (analytes) and is paving its road to real-life applications.[1−3,5,12−18] Any kind of nanostructured noble metal that supports localized surface plasmon resonance (LSPR) and allows enhancement of the Raman signal of the analyte is referred to as the "SERS substrate." Such plasmonic nanostructures can be formed on dielectric, semiconductor, and metal substrates. The bright perspectives of applications have been stimulating ever-growing research on the development and improvement of various types of SERS substrates for their better sensitivity, stability, and lateral uniformity of SERS intensity.[12−14,19−25]

One of the requirements of an efficient SERS substrate of any type is a developed surface (morphology), which not only increases the effective surface area of the sensor but also enables places of close contact between plasmonic nanoparticles (NPs), so-called "hot spots".[19,23,26−32] Various approaches have been proposed to obtain SERS substrates with the highest possible density of the hot spots and their uniform distribution over the substrate surface. Although the best control over the uniformity of the metal nanostructures on the surface and the magnitude of the interparticle distance can be achieved with electron beam lithography,[33] this method is not viable for real-life applications because of the relatively high price. More affordable are methods based on prepatterning[4,34−38] or controlled nucleation of the metallic nanostructures on the surface[35] or methods based on self-assembling.[6,39,40] In the case of self-assembling, the desired morphology can be formed by an oxide or other nonexpensive material and then covered with noble metal.[41−45] Alternatively, the hybrid nanostructures with predefined morphology and plasmonic properties can be first prepared in the solutions and then self-assembled on the substrate to form the hot spots between them.[40,45−54] In most approaches, preparation of

Received: October 24, 2023
Revised: December 29, 2023
Accepted: January 5, 2024
Published: January 18, 2024

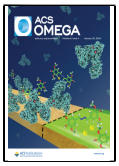

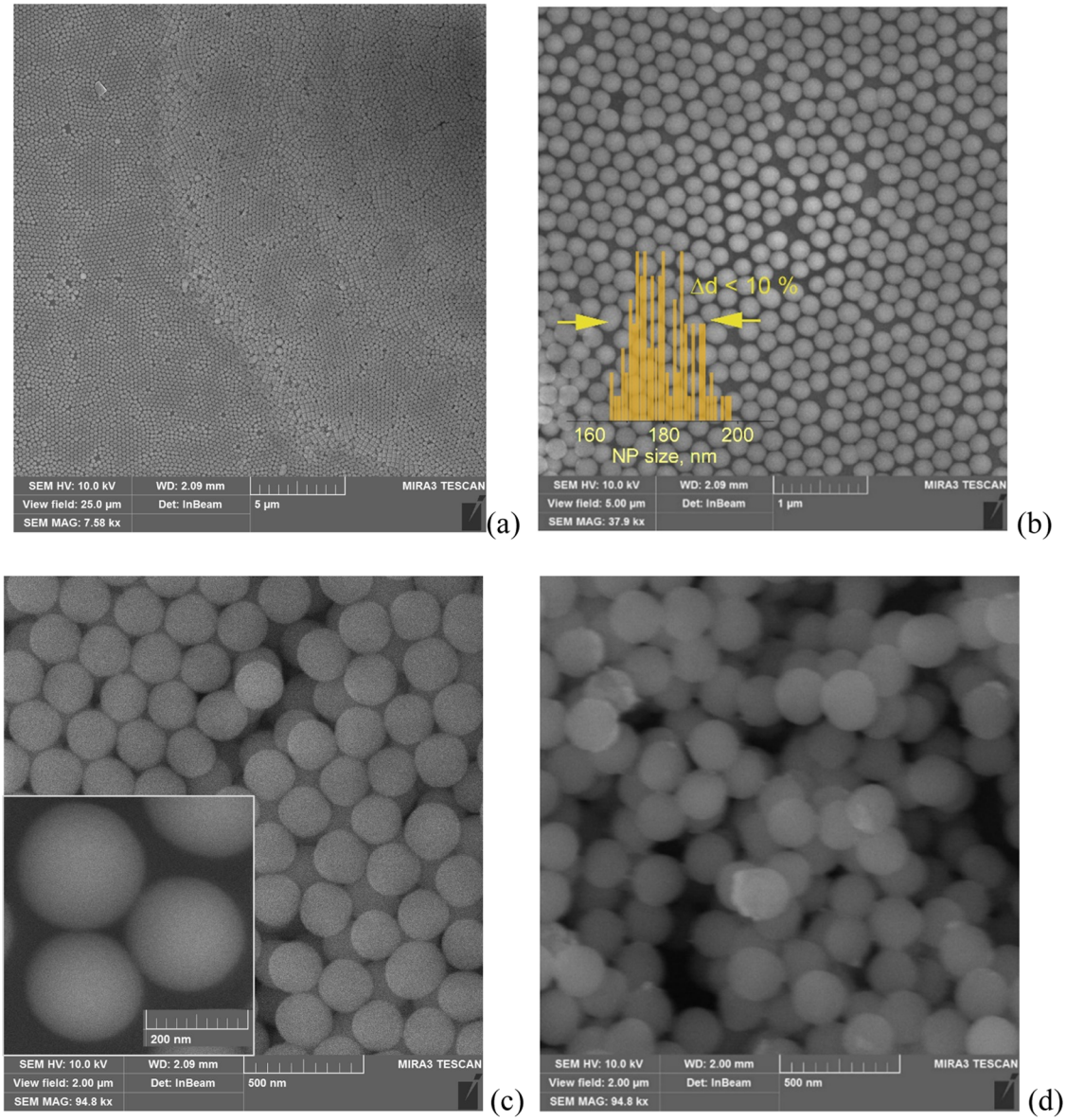

Figure 1. (a–c) SEM images of the self-assembled layers of SiO_2 nanospheres on Si substrate acquired at different magnifications. The scale bar is 5 μm (a), 1 μm (b), and 500 nm (c). Image (d) shows the surface of the layer of SiO_2 nanospheres with the Ag layer of a nominal thickness of 15 nm. The inset in (b) shows the size dispersion of thus prepared nanospheres.

efficient and rigid SERS substrates requires sophisticated and skilled preparation (in the case of nanosphere lithography, for instance) or costly equipment and materials (as in the case of lithographic methods).[35,55] Therefore, affordable fabrication of efficient SERS substrates is still an area of intense research.[7,9,42,55−66] Of particular interest is developing plasmonic architectures that could enable (self-)localization of the analyte in the hot spots.[67]

In this work, we developed efficient SERS substrates based on silica (SiO_2) nanospheres, synthesized by a straightforward route based on the modified Stöbel method,[68] subsequently covered with a thin Ag layer. Annealing of the structure leads to the formation of dense arrays of Ag NPs in the trenches formed by the neighboring silica spheres. Therefore, the resulting morphology is capable of self-localization of the analyte, deposited from the solution, in the same places where hot spots between plasmonic NPs are formed. The advantage of the proposed approach over the technology based on polymer nanospheres[45] is the possibility to anneal the oxide nanosphere substrate in order to tune the plasmonic properties and make the substrate more robust. Previously, silica spheres were used as a basis of the SERS substrate,[48−51,54,69,70] but the approaches were different from the present work. The Ag-decorated silica spheres were assembled into film by a tricky float-and-fishing approach in references;[51,69] however, in the case of complete covering of the spheres with Ag, the portion of Ag NPs that participate in the formation of the hot spots is relatively low, in accordance with another similar study.[52] The approach passed on forming colloidal Au-SiO_2 composites did not show remarkable enhancement,[50,54,71,72] with the best detection limit of only 10^{-7} M. Using microparticles was not efficient,[53,73] assumingly because of the low areal density of the hot spots, which occur between the spheres.

https://doi.org/10.1021/acsomega.3c08393
ACS Omega 2024, 9, 4819−4830

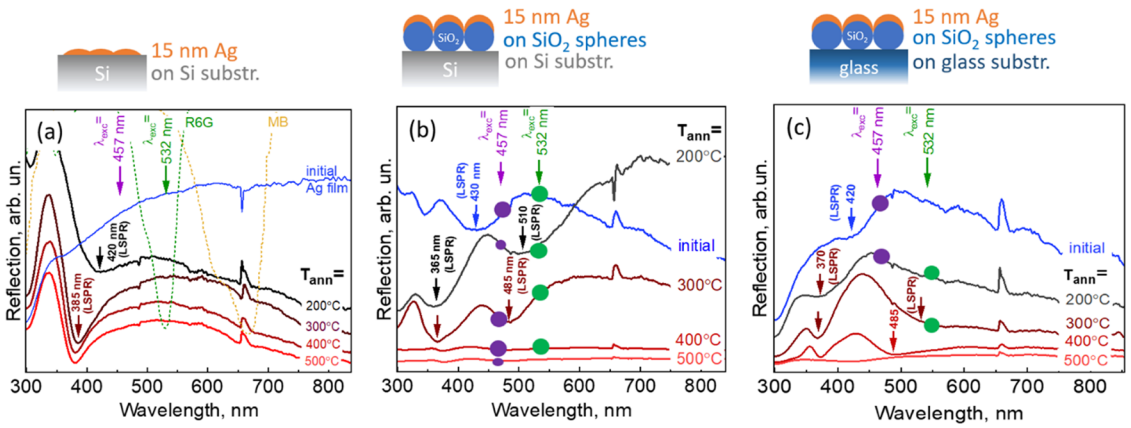

Figure 2. Optical reflection spectra of the structures with a 15 nm Ag film deposited and annealed at different temperatures: on bare Si substrate (a), on SiO_2 nanospheres on Si substrate (b), and on SiO_2 nanospheres on glass substrate (c). Transmission spectra of R6G and CV are shown in (a) to illustrate which of the SERS spectra discussed in the text are resonant. The size of violet and green dots on (b) and (c) is a qualitative measure of SERS intensity for a given combination of substrate and λ_{exc} (shown by arrows) used for taking SERS spectra. In the text of the manuscript, we refer to the minima observed in the transmission or reflection spectra as absorption related to LSPR in the Ag nanostructures. The apparent position of the LSPR bands in the spectra is indicated by arrows.

2. MATERIALS AND METHODS

2.1. Materials. All of the chemical reagents used in our experiments were of analytical grade and used as received without further purification. A precursor solution was prepared from tetraethyl orthosilicate (TEOS: $Si(OC_2H_5)_4$, technical grade, 97%); ethanol (96%) was adopted as the solvent of the precursor. Ammonia (NH_3, 25%) solution was used to increase the pH to promote gelation. H_2O was distilled and deionized. The following materials were used as analytes in SERS experiments: Rhodamine 6G (Sigma-Aldrich), Lysozyme (Sigma-Aldrich), bovine serum albumin (BSA) (Sigma-Aldrich), *Escherichia coli* J5 LPS Monoclonal Antibody (2D7/1), and *Pseudomonas aeruginosa* Monoclonal Antibody (B11) (ThermoFisher Scientific). The analytes were used as purchased, without additional purification of other treatment, only diluted with the deionized water to the required concentration, indicated in the figures.

2.2. Synthesis of SiO_2 Nanospheres and Their Self-Assembling on a Substrate. SiO_2 nanospheres with a narrow size distribution (see Figure 1) were prepared by a sol−gel approach. In particular, it a based on the Stöber method[68] with certain changes. First, two solutions were prepared, "A" and "B" (Figure S1). Solution A was a mixture of TEOS (2 mL) and ethanol (15 mL). Solution B was a mixture of NH_3 (3.6 mL), H_2O (15 mL), and ethanol (16 mL). Solutions A and B were sonicated at 42 kHz separately for 15 min and then mixed and sonicated again for 30 min under ambient conditions. Self-assembling of the SiO_2 nanospheres into ordered layers was achieved by drop casting the colloidal solution onto the clean surface of Si or glass substrates, with its natural drying under ambient conditions. Subsequently, deposition of the Ag layer with a nominal thickness of 15 nm was performed by thermal evaporation in the vacuum of 2×10^{-3} Pa. After annealing for 10 min in Ar atmosphere at a certain temperature (200, 300, 400, or 500 °C), the substrates were cooled down and ready for deposition of the analyte solution (Figure S2).

2.3. Characterization. The morphology of the bare SiO_2 and Ag-covered SiO_2 nanosphere films was studied using scanning electron microscopy (SEM, Tescan Mira 3 MLU). Optical (UV−vis) reflection spectra were obtained using a StellarNet Silver Nova 25 BWI6 spectrometer, which contains tungsten and deuterium lamps as excitation sources. No further instrumental or numerical correction of the spectra was performed. Raman spectra were excited with 457 or 532 nm solid-state lasers and acquired using a single-stage spectrometer MDR-23 (LOMO) equipped with a cooled CCD detector (Andor iDus 420, U.K.). The laser power density on the samples was less than 10^3 W/cm^2 to preclude any thermal or photoinduced modification of the samples. A spectral resolution of 4 cm^{-1} was determined from the Si phonon peak width of a single crystal Si substrate. The Si phonon peak position of 520.5 cm^{-1} was used as a reference for determining the position of the peaks in the Raman/SERS spectra of the analyte.

The analyte was deposited on the SERS substrate by drop casting its solution of a certain concentration indicted for each spectrum or figure. Most of the measurements were performed after the solvent (water) was dried, but some SERS measurements performed from the solution/drop were also performed, and this is specified on the graphs and the corresponding spectra are presented by dashed curves. For the standard analyte (R6G), we estimated the number of molecules probed in the laser spot after the drop-cast sample was allowed to dry. The obtained number of molecules was ∼1000 for the lowest studied R6G concentration of 10^{-13} M.

3. RESULTS AND DISCUSSION

3.1. Morphological and Optical Study. Representative SEM images of the as-synthesized SiO_2 nanospheres self-assembled into ordered layers are shown in Figure 1. As described in Section 2, ordered monolayers of SiO_2 nanospheres synthesized in this work can be formed in the simplest possible way, which is to drop-cast the as-synthesized colloidal suspension onto the substrate without any special treatment and allow it to dry naturally at room temperature.

Along with morphology study, measurement of the spectral position of LSPR is a useful characterization of a SERS substrate, which is necessary for choosing the optimum wavelength of the exciting laser radiation (λ_{exc}) in SERS measurement. Figure 2a shows the optical reflection spectra of 15 nm Ag films on a flat Si substrate (without a layer of SiO_2

https://doi.org/10.1021/acsomega.3c08393
ACS Omega 2024, 9, 4819−4830

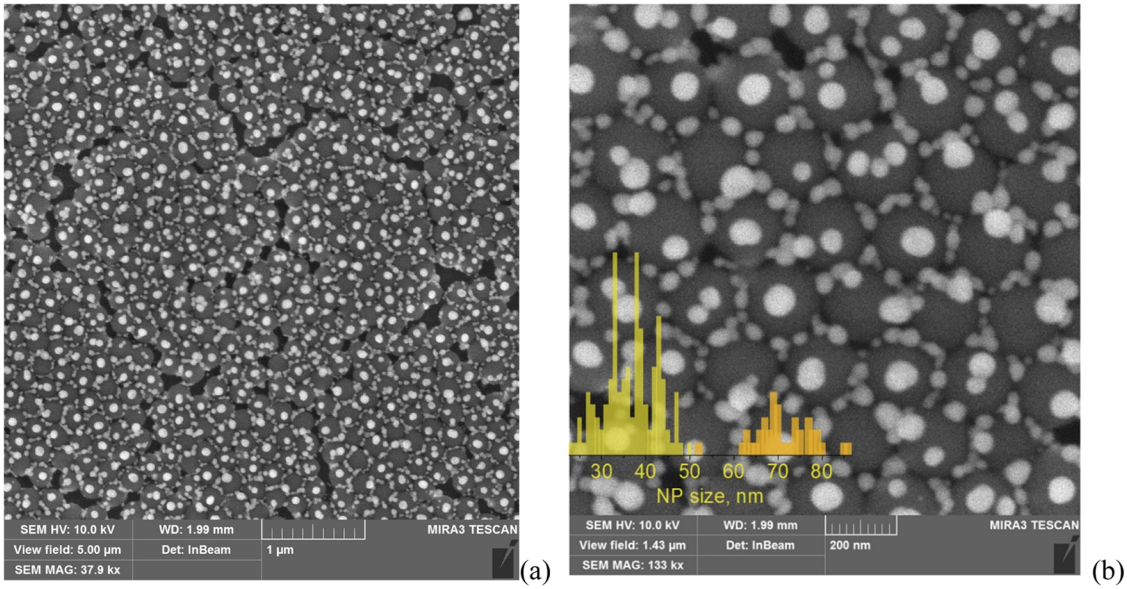

Figure 3. Representative SEM images of the SERS substrates obtained from the Ag film deposited on SiO_2 nanospheres on Si substrate by annealing for 10 min in Ar atmosphere at 300 °C (a,b). The scale bar is 1 μm in (a) and 200 nm in (b). Histogram in (b) shows the bimodal Ag NP distribution.

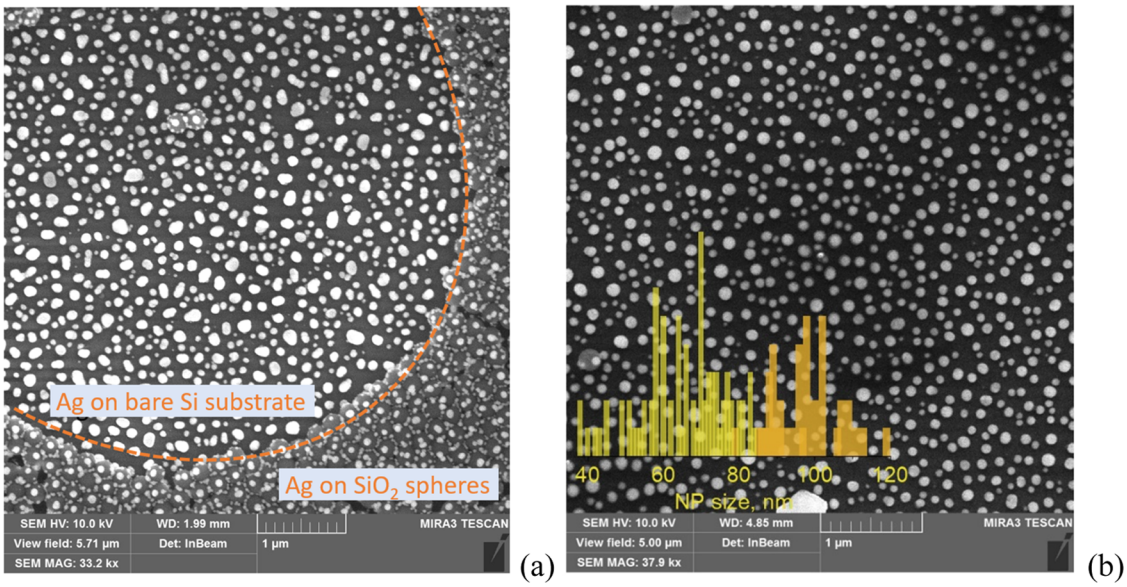

Figure 4. Representative SEM images of SERS substrates in the areas of the Ag film on bare Si substrate (i.e., aside from the self-assembled film of SiO_2 nanospheres): substrate annealed at 300 °C (a) and 500 °C (b). The scale bar is 1 μm. The histogram in (b) shows the Ag NPs size distribution.

spheres) after annealing at different temperatures. The latter series of samples was prepared and studied as a reference in order to underline the striking effect of the SiO_2 nanosphere layer onto the optical spectra of the plasmonic overlayer formed under the same conditions. The transmission spectrum of the as-deposited Ag/Si film does not contain pronounced spectral features, and the film annealed at temperatures up to 200 °C contains a broadband with a minimum centered around 410−415 nm, which is characteristic of LSPR absorption in silver nanostructures of different fabrication routes (colloidal NPs, thermal evaporation, and annealing) and average size.[74−77] For the films annealed at 300 °C, this absorption feature shifts to 385 nm, and only a minor shift to 380 nm occurs at a further increase of the annealing temperature to 400 and 500 °C.

The spectra of the same thickness (15 nm) of Ag deposited on SiO_2 nanospheres on Si and glass substrates (blue curves in Figure 2b,c, respectively) contain an absorption band around 420 nm (Figure 2c) or 430 nm (Figure 2b), similar to the Ag film on flat Si (Figure 2a). The effect of the annealing of the Ag film on SiO_2 spheres on the optical spectra has a principal difference from the same case of flat Si. In addition to the absorption feature in the violet range, which peaked at 365 nm for Ag/SiO_2/Si (Figure 2b) and at 370 nm for Ag/SiO_2/glass (Figure 2c), there appears a distinct absorption band in the blue−green range around 510 nm for T_{ann} = 300 °C and 485 nm for T_{ann} = 400 °C (Figure 2b,c). The only exception from

https://doi.org/10.1021/acsomega.3c08393
ACS Omega 2024, 9, 4819−4830

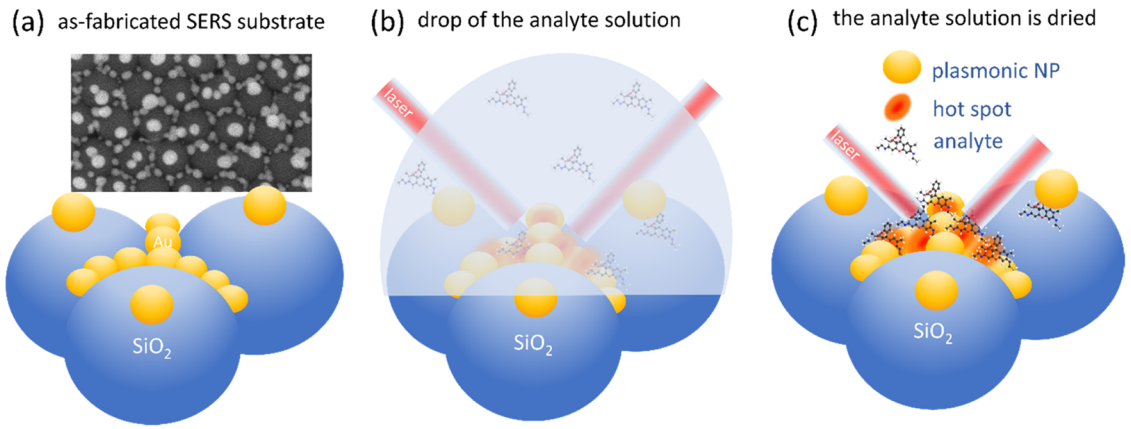

Figure 5. Schematic of SERS substrates and assumed enhancement geometry due to self-localization of the analyte in the hot spots: (a) representative SEM image and schematic of the as-fabricated substrate. (b) Schematic of the hot spot region under laser illumination and deposited drop of the analyte solution. (c) Depictures the same as in (b) but after the solvent is dried.

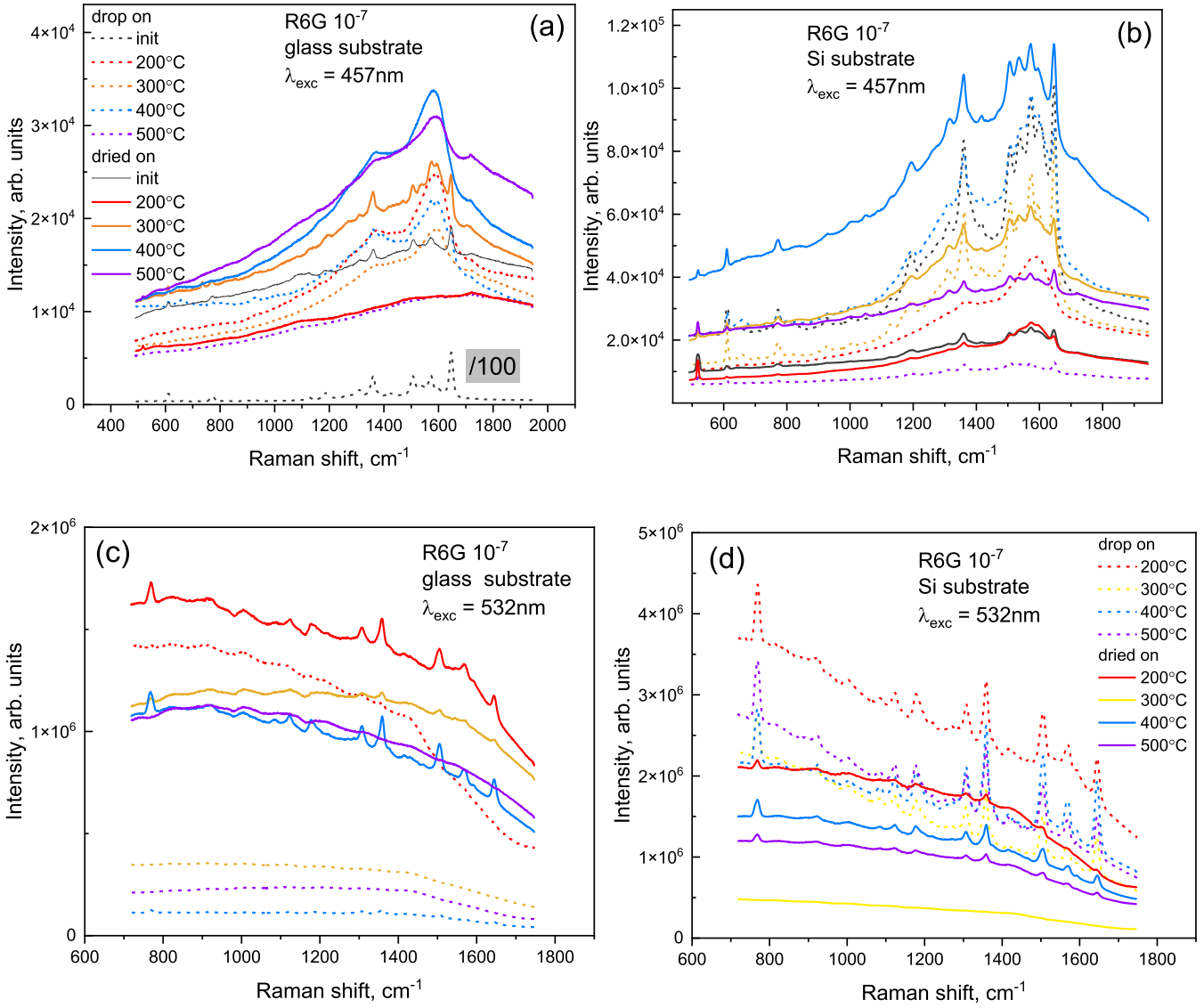

Figure 6. SERS spectra of R6G 10^{-7} M on the SERS substrates formed by the deposition of 15 nm Ag film on SiO_2 nanospheres on Si substrate (b, d) and SiO_2 nanospheres on the glass substrate (a, c) annealed at different temperatures. The spectra obtained at λ_{exc} = 457 nm (a, b) and 532 nm (c, d) from the drop of the solution on the substrate (dash lines) and from the dried drop (solid lines).

https://doi.org/10.1021/acsomega.3c08393
ACS Omega 2024, 9, 4819−4830

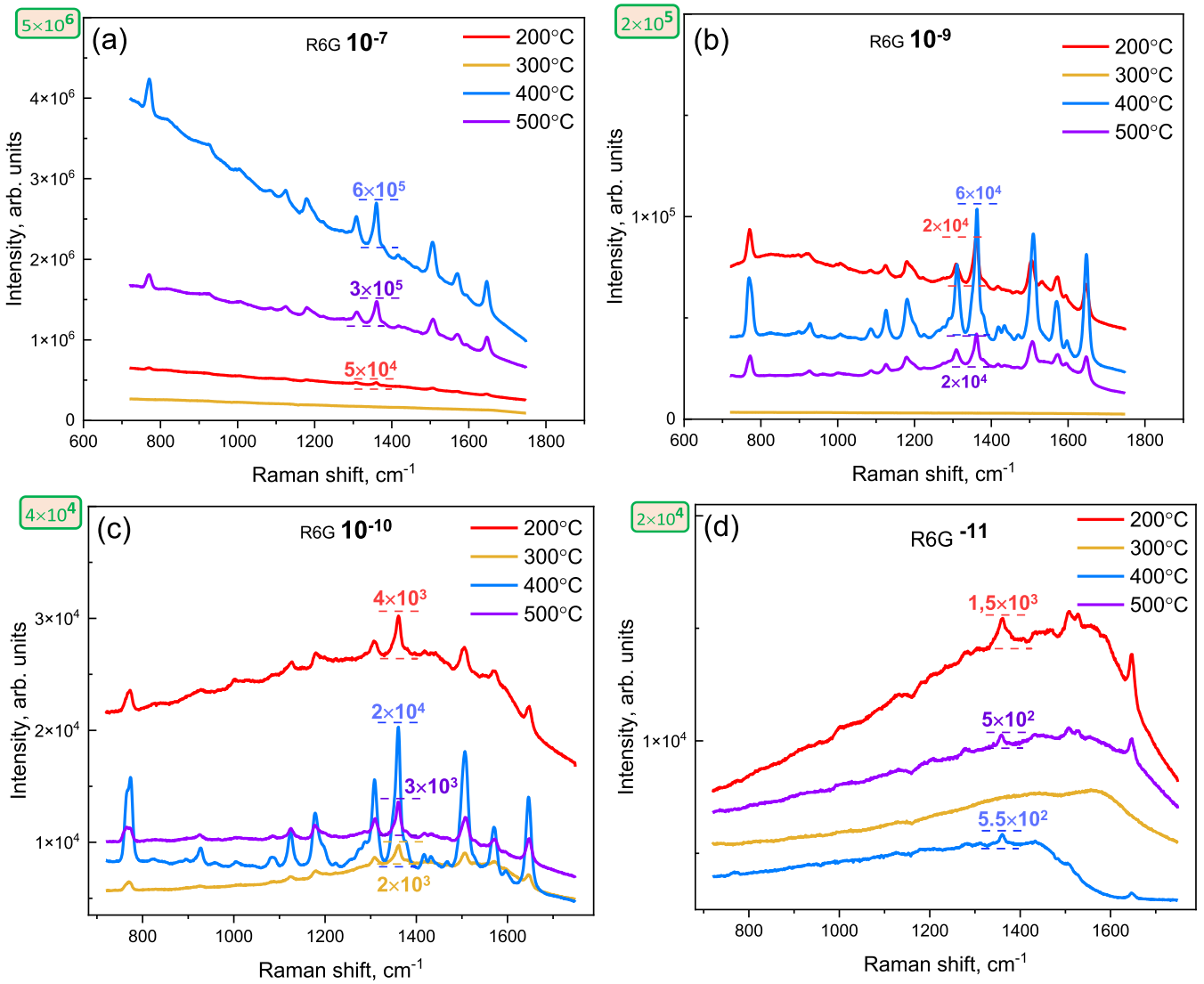

Figure 7. SERS spectra of different concentrations of R6G on the Ag/SiO_2 SERS substrates on Si obtained at different annealing temperatures (indicated on the graphs): (a) 10^{-7} M, (b) 10^{-9} M, (c) 10^{-10} M, and (d) 10^{-11} M. The nominal thickness of Ag is 15 nm, and the spectra are obtained at λ_{exc}= 532 nm from the dried analyte. The intensity of the 1360 cm^{-1} peak is shown in each spectrum.

this trend is the substrate on glass annealed at 500 °C, it contains a single band around 430 nm, similar to the as-deposited film (Figure 2b,c). Note that all of the observed evolution of the optical spectra are related to plasmonic nanoparticles but not to the silica spheres because the spectra of the latter do not show noticeable changes in the same range of annealing temperatures (Figure S3).

Inspection of the SEM images of the annealed samples revealed the general trend for the plasmonic structures on SiO_2 spheres (Figures 3 and S4), a bimodal formation of Ag nanoparticles (NPs), with a regular distribution of the surface of the SERS substrate. One type is NPs about 60−80 nm, situated on top of SiO_2 spheres, predominantly one NP per sphere. The second type is 30−40 nm NPs located in the trenches between the SiO_2 spheres (see the histogram in the inset of Figure 3b).

One could assume that two absorption bands in the UV−vis spectra can be related to these two size distributions of NPs. However, the annealed Ag film on flat Si shows a bimodal distribution of Ag NPs (Figure 4); however, in the UV−vis spectra, only one absorption peak is observed (Figure 2a). Important is that the UV−vis spectra (Figure 2a) and SEM images (Figure 4) of Ag on bare Si were acquired on the very same samples as the spectra and images with SiO_2 nanospheres (e.g., see Figure 4a), i.e., the Ag deposition and annealing conditions were exactly the same. Therefore, we can come to an important preliminary conclusion that the additional absorption band in the blue−green range in the spectra of annealed Ag/SiO_2 structures is not due to one of two size fractions of the Ag NPs but due to NPs that are in contact with each other, i.e., those that presumably form hot spots. It has been repeatedly proven in the literature that interaction between individual plasmonic NPs shifts the LSPR significantly to longer wavelengths.[74−77] Therefore, the violet band (between 350 and 400 nm) observed in our UV−vis spectra (Figure 2b,c) is due to individual NPs, and the blue−green one (between 450 and 550 nm) is due to interacting NPs, i.e., NPs situated in the trenches formed by neighboring SiO_2 spheres. One can expect that excitation of the Raman spectra within the absorption band related to NPs forming the hot spots will result in a high efficiency of the SERS spectra. It should be noted that an efficient SERS substrate does not necessarily

https://doi.org/10.1021/acsomega.3c08393
ACS Omega 2024, 9, 4819−4830

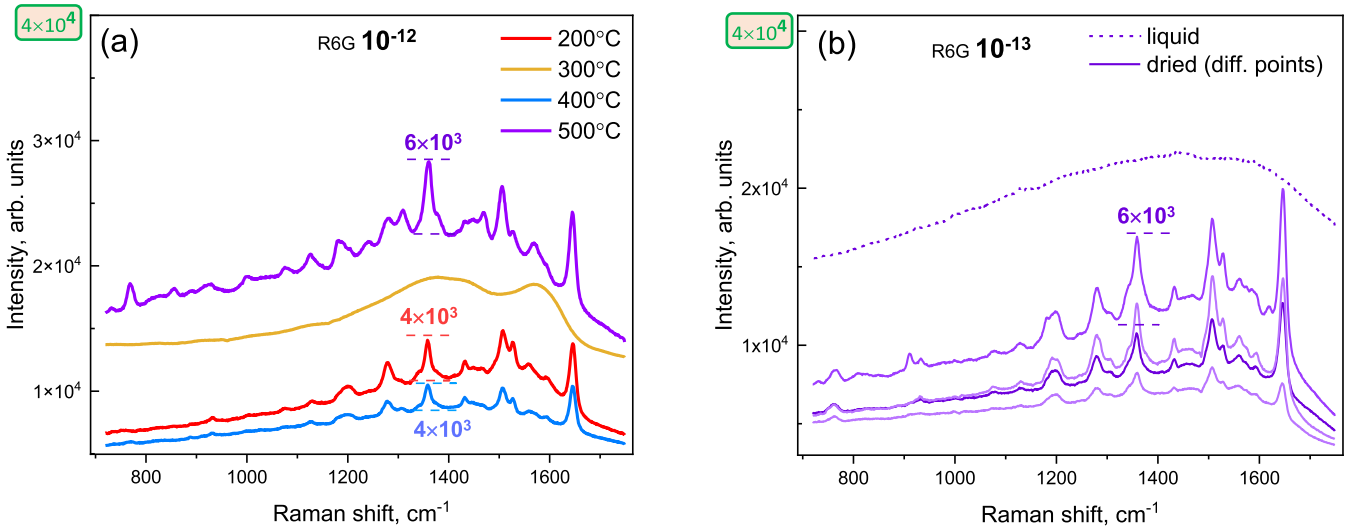

Figure 8. (a) SERS spectra of dried 10^{-12} M R6G on Ag/SiO_2 SERS substrates on Si obtained at different annealing temperatures (indicated on the graphs). (b) SERS spectra of 10^{-13} M R6G on Ag/SiO_2 SERS substrates on Si obtained at an annealing temperature of 500 °C, measured from the drop and different points of the dried solution.

exhibit sharp peaks due to plasmonic resonance, but a gradient (spectral) distribution of multiple localized resonances[78] or coupling/additive effect of localized plasmon and polariton[79] can be advantageous for high SERS intensity.

In addition to the hot spot effect, the (resonant) excitation of the NPs situated in the trenches is expected to result in a strong SERS signal because this is the same location where the concentration (enrichment) of the analyte molecules can be expected. Therefore, the developed technology of the SERS substrate fabrication ensures simultaneous several key conditions of an efficient SERS (Figure 5): (i) self-organization of the metal NPs into hot spots; (ii) enrichment/concentration of the analyte in the hot spots; (iii) shift of the Ag LSPR to the range where a larger number of laser lines are available and CCD detectors are more sensitive. In addition, the proposed morphology is beneficiary for a homogeneous lateral distribution of the analyte solution and avoids the known problem of the coffee-ring effect.[80]

In the following section, we studied in detail the SERS efficiency of the developed substrates, using different excitations and analyte concentrations and compared analytes in solution and dried.

3.2. SERS Characterization. Figure 6 shows the SERS spectra of 10^{-7} M solution of R6G, measured on SERS substrates fabricated on glass and Si and subject to different annealing temperatures. A general trend that can be noticed is that the substrates on Si are more efficient, almost every substrate exhibits enhancement for both solution and dried analyte, and the average magnitude of the SERS signal is larger than for substrates on glass. This can be related to a denser packing of the SiO_2 spheres on Si compared to glass. Because of the poor wetting of the water solution of the Si surface, the drop with SiO_2 spheres does not spread over the surface during drying, and the nanospheres assemble in more tightly packed structures. On the glass, an opposite situation takes place wherein the drop of water solution with SiO_2 nanospheres spreads over the surface.

This may result in less dense packing of the spheres; thus, a smaller number of hot spots are formed after Ag deposition and annealing. Noteworthy is that the high(er) SERS intensity observed in our spectra does not necessarily correlate with the (high) plasmon absorption in the UV−vis spectra. This is especially pronounced for the SERS substrates obtained in this work on the glass; at λ_{exc} = 457 nm, the SERS is observed on initial (not annealed) and 300 °C annealed structures on glass (Figure 6a), which do not exhibit absorption features close to this λ_{exc} (Figure 2). On the contrary, the latter sample even has a dip in absorption at 457 nm. The sample on glass that has a distinct absorption (centered around 490 nm) is the one annealed at 400 °C, but this substrate is not efficient at 457 nm, only at 532 nm, although both λ_{exc}'s are inside the absorption band. At the same time, at 532 nm, SERS is also observed for the 200 °C substrate on the glass, which does not possess distinct absorption in the green range (Figure 2). Therefore, one can conclude that such a poor correlation between the SERS intensity and resonance conditions of λ_{exc} with plasmon absorption can indicate that for the type of SERS substrates under study, the enhancement is determined by the hot spots. The absence of distinct absorption features in the UV−vis spectra of the efficient substrates can be related to the significant distribution of their spectral properties and the concomitant broadening of the absorption spectra/features.[78] Noteworthy is that in many works devoted to SERS, the optical absorption/reflection spectra are not reported.[81]

An important observation can be made from a comparison of the Raman spectra acquired from different concentrations of R6G on the same set of substrates (Figures 7 and 8). First, with the decrease in concentration from 10^{-7} to 10^{-9} M, the amplitude of the Raman peaks decreases only by 1 order of magnitude and the PL background weakens significantly. After two further steps of concentration decrease, down to 10^{-11} M, a decrease in the Raman peak magnitude is still smaller than a drop in concentration. Also, at 10^{-12} M, the SERS intensity is surprisingly higher than at 10^{-11} M.

From the above observations, we can make an important conclusion regarding the mechanism of the Raman enhancement in the system and the interplay between the Raman and PL contributions to the spectra. In the previous works on SERS of fluorescent molecules (dyes), the ratio of the PL and Raman peak intensity in the SERS experiments has been

https://doi.org/10.1021/acsomega.3c08393
ACS Omega 2024, 9, 4819−4830

shown to be proportional (average) to the distance between the plasmonic nanoparticle and analyte molecule.[82,83] Therefore, in our case, at a relatively high analyte concentration, presumably $\geq 10^{-7}$ M for our type of substrates, the number of analyte molecules is much larger than the number of hot spots (which is constant for the given substrate). As a result, only a small fraction of the molecules gets located in the hot spots, where their Raman spectrum is greatly enhanced and PL is quenched. The rest of the molecules are located away from the hot spots (either laterally aside or as subsequent layers on top of the molecule sitting right in the hot spot), their Raman contribution is not or weakly enhanced and PL is not quenched. With the decrease of the analyte concentration by 2 orders of magnitude (to 10^{-9} M), the PL background decreases drastically, while the magnitude and Raman peak amplitude change by less than an order of magnitude.

This behavior indicates that the reduction of the concentration of the deposited analyte molecules led to a reduction of the number of molecules that are not in the hot spots, while the number of the molecules in the hot spots is changing less significantly. This conclusion is an important argument that the strategy of analyte self-localization in the hot spots has been successfully implemented in the type of SERS substrate developed in our work. The latter conclusion is additionally confirmed by a slow decrease and even the reversed increase of the Raman intensity at extremely low R6G concentration of 10^{-11} to 10^{-13} M (Figure 9). Apparently, in this concentration step, the number of analyte molecules became comparable to (or even smaller than) the number of hot spots. Therefore, the net intensity in the SERS spectrum is very sensitive to the particular conditions of the analyte depositions, drying, and final configuration of the analyte distribution on the surface. The enhancement factor estimated from comparison with the intensity regular Raman (non-SERS) peaks ($\sim 10^3$) of 10^{-5} M R6G (Figure S5a,b) is $\sim 10^8$.

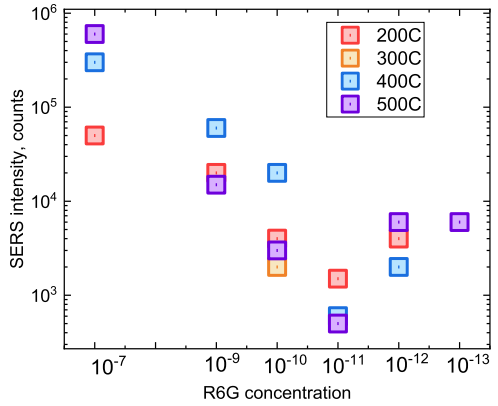

Figure 9. Dependence of SERS intensity on concentrations of R6G on the Ag/SiO_2 SERS substrates obtained at different annealing temperatures (based on the spectra in Figures 7 and 8).

Although the detailed study described above was performed only with one molecule, R6G, different other molecules were studied on the SERS substrates developed in this work, particularly the biomolecules such as lysozyme, BSA (bovine serum albumin), or antibodies (Figure 10), for which λ_{exc} = 532 nm is not resonant and regular Raman spectra are not detectable (Figure S5c,d).

Both the approach to fabrication and the final morphology of SERS substrates developed in this work have not been reported in the literature before. The seemingly close approach, "film-over-nanosphere" (FON), is to cover the noble metal with a layer of polystyrene (PS) nanospheres,[28,41,45] which does not allow annealing of such a structure. Moreover, assembling the PS spheres into layers is a much more time-consuming process. In the only work,[84] that has employed SiO_2 spheres in a similar approach (unfortunately, the synthesis of the SiO_2 nanospheres was not described) has used a much larger nominal thickness of Ag, up to 200 nm, and no annealing was applied. Consequently, a completely different morphology of the metal layer was obtained in ref[84]84. Notably, in the latter work, the SERS spectra (λ_{exc} = 532 nm) of roughly the same intensity (S/N ratio) were observed for a very broad range of R6G concentrations, from 10^{-6} to 10^{-10} M. This observation is similar to our results for the concentration range 10^{-10} to 10^{-13} M (Figure 8) and additionally confirms our assumption that the SERS intensity in this type of SERS substrates is determined by the hot spots. In ref 85, Ag and Au NPs were formed on the SiO_2 layer using an expensive setup focusing on metal cluster fabrication and homogeneous deposition on a substrate. The SiO_2 layer formation was also not straightforward, it employed a vertical deposition method on Piranha solution-cleaned Si substrates. Interestingly, λ_{exc} = 785 nm was used for both Ag- and Au-based SERS substrates in ref 85. Unfortunately, in the simulations of the electric field distribution performed for the plasmonic structures developed in ref 85, the wavelength was not mentioned. A representative comparative analysis of the resonant behavior of the SERS substrates developed in this work with similar structures in the literature is not possible at the moment because no UV−vis spectra have usually been shown for FON-type SERS substrates reported in the literature.[84,85] Moreover, for none of the FON-type SERS substrates reported in the literature, the metal overlayer was subject to annealing (because PS spheres do not withstand the high temperatures needed to change the morphology of gold or silver film). In ref 86, one of a few works that have used ordered SiO_2 spheres as a basis of a SERS substrate, the UV−vis spectra of the sputtering-deposited Ag onto SiO_2 nanosphere monolayer were not much structured: no distinct feature for 10 nm Ag and a single broadband at 480 nm for 20 nm Ag and at 511 nm for 30 nm Ag. For the two known works, where silica spheres were used as a basis of the SERS substrate,[51,69] the achieved sensitivity was much lower than in the present work, e.g., 10^{-12} M R6G in ref 69.

4. CONCLUSIONS

We have developed a straightforward fabrication method of efficient SERS substrates, which includes an original one-step synthesis of highly monodisperse SiO_2 spheres at room temperature, their quick self-assembling on the deliberate substrate, thermal evaporation of a few-nanometer (15 nm) Ag layer. The as-obtained SERS substrate is already quite efficient at λ_{exc} = 457 nm, but its efficiency is greatly improved and resonance excitation shifted to λ_{exc} = 532 nm by a short-time annealing under an Ar_2 atmosphere. The substrates developed allow Rhodamine 6G concentrations down to 10^{-13} M to be easily detected. Good efficiency for nonresonant analytes, in particular, lysozyme and other biomolecules, is also demonstrated. Scanning electron microscopy study unveils the reason for the high efficiency of the developed SERS substrate, the obtained morphology allows the formation of numerous hot spots in the places of expected localization (enrichment) of the

https://doi.org/10.1021/acsomega.3c08393
ACS Omega 2024, 9, 4819−4830

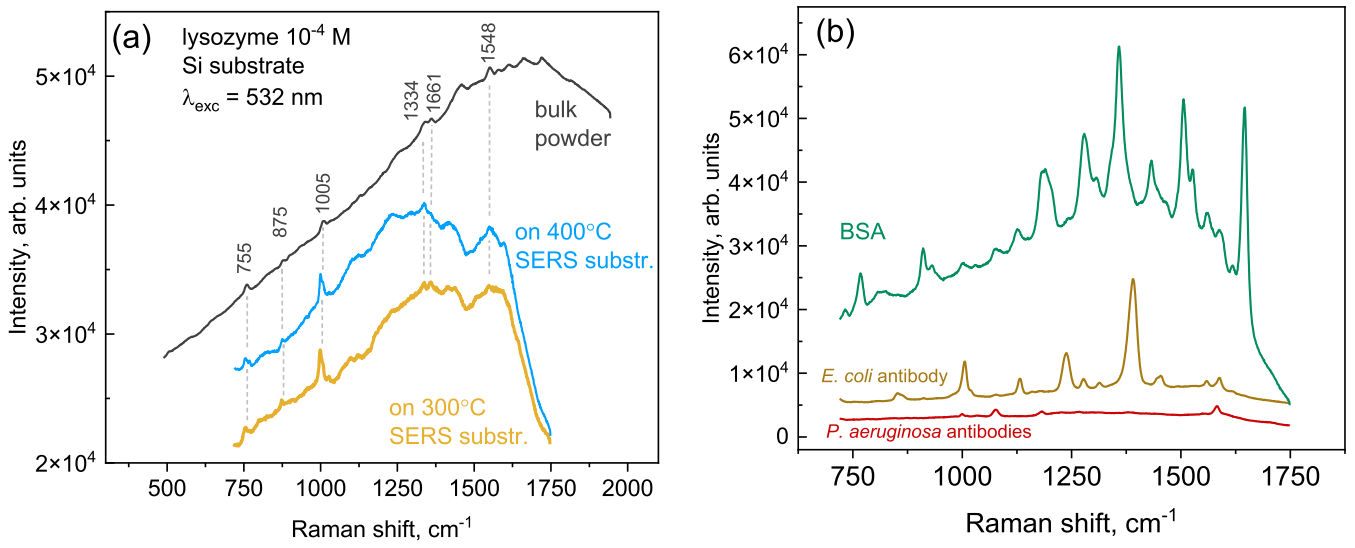

Figure 10. (a) SERS spectra of 10^{-4} M lysozyme solution dried on the SERS substrates formed by the deposition of 15 nm Ag film SiO_2 nanospheres on Si and annealing at 300 °C or 400 °C (λ_{exc}= 532 nm). The spectrum of bulk lysozyme was measured as a reference (λ_{exc} = 457 nm). (b) SERS spectra of 10^{-4} M BSA and of *P. aeruginosa* and *E. coli* antibodies.

analyte during solvent drying in the trenches between SiO_2 spheres. Moreover, this morphology presumably reduces the negative effects of thermophoresis that may otherwise push the analyte away from the hot spots and is only rarely considered in the context of SERS works. The effect of plasmonic NPs on the quenching of analyte fluorescence as a factor of apparent SERS intensity is also discussed.

■ ASSOCIATED CONTENT

Data Availability Statement

Data will be made available on request.

Supporting Information

The Supporting Information is available free of charge at https://pubs.acs.org/doi/10.1021/acsomega.3c08393.

Schematic of the fabrication process (Figure S1), photograph of the as-prepared SERS substrate (Figure S2), optical reflection spectra of the bare SiO_2 spheres (Figure S3), SEM images of the SERS substrates obtained by annealing at 500 °C (Figure S4), and Raman spectra of the analytes (Figure S5) (PDF)

■ AUTHOR INFORMATION

Corresponding Author

Volodymyr Dzhagan − *V. Lashkaryov Institute of Semiconductors Physics, National Academy of Sciences of Ukraine, Kyiv 03028, Ukraine; Physics Department, Taras Shevchenko National University of Kyiv, Kyiv 01601, Ukraine;* orcid.org/0000-0002-7839-9862; Email: dzhagan@isp.kiev.ua

Authors

Nazar Mazur − *V. Lashkaryov Institute of Semiconductors Physics, National Academy of Sciences of Ukraine, Kyiv 03028, Ukraine*

Olga Kapush − *V. Lashkaryov Institute of Semiconductors Physics, National Academy of Sciences of Ukraine, Kyiv 03028, Ukraine*

Mykola Skoryk − *G. V. Kurdyumov Institute for Metal Physics, National Academy of Sciences of Ukraine, Kyiv 03142, Ukraine*

Yaroslav Pirko − *Institute of Food Biotechnology and Genomics, National Academy of Sciences of Ukraine, Kyiv 04123, Ukraine*

Alla Yemets − *Institute of Food Biotechnology and Genomics, National Academy of Sciences of Ukraine, Kyiv 04123, Ukraine*

Vladyslav Dzhahan − *Physics Department, Taras Shevchenko National University of Kyiv, Kyiv 01601, Ukraine*

Petro Shepeliavyi − *V. Lashkaryov Institute of Semiconductors Physics, National Academy of Sciences of Ukraine, Kyiv 03028, Ukraine*

Mykhailo Valakh − *V. Lashkaryov Institute of Semiconductors Physics, National Academy of Sciences of Ukraine, Kyiv 03028, Ukraine*

Volodymyr Yukhymchuk − *V. Lashkaryov Institute of Semiconductors Physics, National Academy of Sciences of Ukraine, Kyiv 03028, Ukraine*

Complete contact information is available at: https://pubs.acs.org/10.1021/acsomega.3c08393

Author Contributions

The manuscript was written through the contributions of all authors. V. Dzhagan wrote the original draft and performed project administration and visualization. N.M., O.K., M.S., Y.P., V. Dzhahan, and P.S. performed the investigation and data curation. V.Y. was responsible for conceptualization, funding acquisition, formal analysis, and methodology. M.V. and A.Y. wrote, reviewed, and edited the manuscript and supervised the study. All authors have given approval to the final version of the manuscript.

Funding

Financial support from the National Research Foundation of Ukraine is greatly acknowledged under Project No. 2020.02/0204 for V. Dzhagan, N.M., O.K., Y.P., and V.Y.

Notes

The authors declare no competing financial interest.

REFERENCES

(1) Shi, L.; Zhang, L.; Tian, Y. Rational Design of Surface-Enhanced Raman Scattering Substrate for Highly Reproducible Analysis. *Anal. Sens.* **2023**, *3* (2), No. e202200064.

(2) Moisoiu, T.; Dragomir, M. P.; Iancu, S. D.; Schallenberg, S.; Birolo, G.; Ferrero, G.; Burghelea, D.; Stefancu, A.; Cozan, R. G.; Licarete, E.; Allione, A.; Matullo, G.; Iacob, G.; Bálint, Z.; Badea, R. I.; Naccarati, A.; Horst, D.; Pardini, B.; Leopold, N.; Elec, F. Combined MiRNA and SERS Urine Liquid Biopsy for the Point-of-Care Diagnosis and Molecular Stratification of Bladder Cancer. *Mol. Med.* **2022**, *28* (1), No. 39.

(3) Moisoiu, V.; Iancu, S. D.; Stefancu, A.; Moisoiu, T.; Pardini, B.; Dragomir, M. P.; Crisan, N.; Avram, L.; Crisan, D.; Andras, I.; Fodor, D.; Leopold, L. F.; Socaciu, C.; Bálint, Z.; Tomuleasa, C.; Elec, F.; Leopold, N. SERS Liquid Biopsy: An Emerging Tool for Medical Diagnosis. *Colloids Surf., B* **2021**, *208*, No. 112064.

(4) Chursanova, M. V.; Dzhagan, V. M.; Yukhymchuk, V. O.; Lytvyn, O. S.; Valakh, M. Y.; Khodasevich, I. A.; Lehmann, D.; Zahn, D. R. T.; Waurisch, C.; Hickey, S. G. Nanostructured Silver Substrates with Stable and Universal Sers Properties: Application to Organic Molecules and Semiconductor Nanoparticles. *Nanoscale Res. Lett.* **2010**, *5* (2), 403.

(5) Usha, S. P.; Manoharan, H.; Deshmukh, R.; Álvarez-Diduk, R.; Calucho, E.; Sai, V. V. R.; Merkoçi, A. Attomolar Analyte Sensing Techniques (AttoSens): A Review on a Decade of Progress on Chemical and Biosensing Nanoplatforms. *Chem. Soc. Rev.* **2021**, *50*, 13012−13089.

(6) Ionescu, R. E.; Aybeke, E. N.; Bourillot, E.; Lacroute, Y.; Lesniewska, E.; Adam, P. M.; Bijeon, J. L. Fabrication of Annealed Gold Nanostructures on Pre-Treated Glow-Discharge Cleaned Glasses and Their Used for Localized Surface Plasmon Resonance (LSPR) and Surface Enhanced Raman Spectroscopy (SERS) Detection of Adsorbed (Bio)Molecules. *Sensors* **2017**, *17* (2), 236.

(7) Mikoliunaite, L.; Rodriguez, R. D.; Sheremet, E.; Kolchuzhin, V.; Mehner, J.; Ramanavicius, A.; Zahn, D. R. T. The Substrate Matters in the Raman Spectroscopy Analysis of Cells. *Sci. Rep* **2015**, *5*, No. 13150.

(8) Muntean, C. M.; Leopold, N.; Halmagyi, A.; Valimareanu, S. Surface-Enhanced Raman Scattering Assessment of DNA from Leaf Tissues Adsorbed on Silver Colloidal Nanoparticles. *J. Raman Spectrosc.* **2013**, *44* (6), 817−822.

(9) Malek, K.; Jaworska, A.; Krala, P.; Kachamakova-Trojanowska, N.; Baranska, M. Imaging of Macrophages by Surface Enhanced Raman Spectroscopy (SERS). *Biomed. Spectrosc. Imaging* **2013**, *2* (4), 349−357.

(10) Lughi, V.; Bonifacio, A.; Barbone, M.; Marsich, L.; Sergo, V. Surface-Enhanced Raman Effect in Hybrid Metal-Semiconductor Nanoparticle Assemblies. *J. Nanopart. Res.* **2013**, *15* (5), 1663.

(11) Muravitskaya, A.; Rumyantseva, A.; Kostcheev, S.; Dzhagan, V.; Stroyuk, O.; Adam, P.-M. Enhanced Raman Scattering of ZnO Nanocrystals in the Vicinity of Gold and Silver Nanostructured Surfaces. *Opt. Express* **2016**, *24* (2), A168.

(12) Fornasaro, S.; Alsamad, F.; Baia, M.; Batista De Carvalho, L. A. E.; Beleites, C.; Byrne, H. J.; Chiadò, A.; Chis, M.; Chisanga, M.; Daniel, A.; Dybas, J.; Eppe, G.; Falgayrac, G.; Faulds, K.; Gebavi, H.; Giorgis, F.; Goodacre, R.; Graham, D.; La Manna, P.; Laing, S.; Litti, L.; Lyng, F. M.; Malek, K.; Malherbe, C.; Marques, M. P. M.; Meneghetti, M.; Mitri, E.; Mohaček-Grošev, V.; Morasso, C.; Muhamadali, H.; Musto, P.; Novara, C.; Pannico, M.; Penel, G.; Piot, O.; Rindzevicius, T.; Rusu, E. A.; Schmidt, M. S.; Sergo, V.; Sockalingum, G. D.; Untereiner, V.; Vanna, R.; Wiercigroch, E.; Bonifacio, A. Surface Enhanced Raman Spectroscopy for Quantitative Analysis: Results of a Large-Scale European Multi-Instrument Interlaboratory Study. *Anal. Chem.* **2020**, *92* (5), 4053−4064.

(13) Aitchison, H.; Aizpurua, J.; Arnolds, H.; Baumberg, J.; Bell, S.; Bonifacio, A.; Chikkaraddy, R.; Dawson, P.; De Nijs, B.; Deckert, V.; Delfino, I.; Di Martino, G.; Eremina, O.; Faulds, K.; Fountain, A.; Gawinkowski, S.; Gomez Castano, M.; Goodacre, R.; Gracie, J.; Graham, D.; Guicheteau, J.; Hardwick, L.; Hardy, M.; Heck, C.; Jamieson, L.; Kamp, M.; Keeler, A.; Kuttner, C.; Langer, J.; Mahajan, S.; Martín Sabanés, N.; Murakoshi, K.; Porter, M.; Schatz, G.; Schlücker, S.; Tian, Z.; Tripathi, A.; Van Duyne, R.; Vikesland, P. Analytical SERS: General Discussion. *Faraday Discuss.* **2017**, *205*, 561−600.

(14) Grys, D. B.; de Nijs, B.; Huang, J.; Scherman, O. A.; Baumberg, J. J. SERSbot: Revealing the Details of SERS Multianalyte Sensing Using Full Automation. *ACS Sens.* **2021**, *6* (12), 4507−4514.

(15) Itoh, T.; Procházka, M.; Dong, Z. C.; Ji, W.; Yamamoto, Y. S.; Zhang, Y.; Ozaki, Y. Toward a New Era of SERS and TERS at the Nanometer Scale: From Fundamentals to Innovative Applications. *Chem. Rev.* **2022**, *123*, 1552−1634.

(16) Buja, O. M.; Gordan, O. D.; Leopold, N.; Morschhauser, A.; Nestler, J.; Zahn, D. R. T. Microfluidic Setup for On-Line SERS Monitoring Using Laser Induced Nanoparticle Spots as SERS Active Substrate. *Beilstein J. Nanotechnol.* **2017**, *8* (1), 237−243.

(17) Son, W. K.; Choi, Y. S.; Han, Y. W.; Shin, D. W.; Min, K.; Shin, J.; Lee, M. J.; Son, H.; Jeong, D. H.; Kwak, S. Y. In Vivo Surface-Enhanced Raman Scattering Nanosensor for the Real-Time Monitoring of Multiple Stress Signalling Molecules in Plants. *Nat. Nanotechnol.* **2023**, *18* (2), 205−216.

(18) Zheng, D.; Pisano, F.; Collard, L.; Balena, A.; Pisanello, M.; Spagnolo, B.; Mach-Batlle, R.; Tantussi, F.; Carbone, L.; De Angelis, F.; Valiente, M.; de la Prida, L. M.; Ciracì, C.; De Vittorio, M.; Pisanello, F. Toward Plasmonic Neural Probes: SERS Detection of Neurotransmitters through Gold-Nanoislands-Decorated Tapered Optical Fibers with Sub-10 Nm Gaps. *Adv. Mater.* **2023**, *35* (11), No. 2200902.

(19) Novara, C.; Dalla Marta, S.; Virga, A.; Lamberti, A.; Angelini, A.; Chiadò, A.; Rivolo, P.; Geobaldo, F.; Sergo, V.; Bonifacio, A.; Giorgis, F. SERS-Active Ag Nanoparticles on Porous Silicon and PDMS Substrates: A Comparative Study of Uniformity and Raman Efficiency. *J. Phys. Chem. C* **2016**, *120* (30), 16946−16953.

(20) Dvoynenko, M. M.; Wang, H. H.; Liu, C. Y.; Wang, Y. L.; Wang, J. K. Retrieving Plasmonic Enhancement Factor with Optical Thermometry. *J. Phys. Chem. C* **2020**, *124* (50), 27673−27679.

(21) Klestova, Z. S.; Voronina, A. K.; Yushchenko, A. Y.; Vatlitsova, O. S.; Dorozinsky, G. V.; Ushenin, Y. V.; Maslov, V. P.; Doroshenko, T. P.; Kravchenko, S. A. Aspects of "Antigen−Antibody" Interaction of Chicken Infectious Bronchitis Virus Determined by Surface Plasmon Resonance. *Spectrochim. Acta, Part A* **2022**, *264*, No. 120236.

(22) Cialla, D.; Pollok, S.; Steinbrücker, C.; Weber, K.; Popp, J. SERS-Based Detection of Biomolecules. *Nanophotonics* **2014**, *3* (6), 383−411.

(23) Shiohara, A.; Wang, Y.; Liz-Marzán, L. M. Recent Approaches toward Creation of Hot Spots for SERS Detection. *J. Photochem. Photobiol. C* **2014**, *21*, 2−25.

(24) Mikac, L.; Ivanda, M.; Gotić, M.; Mihelj, T.; Horvat, L. Synthesis and Characterization of Silver Colloidal Nanoparticles with Different Coatings for SERS Application. *J. Nanopart. Res.* **2014**, *16* (12), No. 2748.

(25) Iancu, S. D.; Stefancu, A.; Moisoiu, V.; Leopold, L. F.; Leopold, N. The Role of Ag+, Ca2+, Pb2+ and Al3+ Adions in the SERS Turn-on Effect of Anionic Analytes. *Beilstein J. Nanotechnol.* **2019**, *10*, 2338−2345.

(26) Kleinman, S. L.; Frontiera, R. R.; Henry, A.-I.; Dieringer, Ja.; Van Duyne, R. P. Creating, Characterizing, and Controlling Chemistry with SERS Hot Spots. *Phys. Chem. Chem. Phys.* **2013**, *15*, 21−36.

(27) Stefancu, A.; Iancu, S. D.; Leopold, N. Selective Single Molecule SERRS of Cationic and Anionic Dyes by Cl-and Mg2+Adions: An Old New Idea. *J. Phys. Chem. C* **2021**, *125* (23), 12802−12810.

(28) Farcau, C.; Astilean, S. Mapping the SERS Efficiency and Hot-Spots Localization on Gold Film over Nanospheres Substrates. *J. Phys. Chem. C* **2010**, *114* (27), 11717−11722.

(29) Hakonen, A.; Svedendahl, M.; Ogier, R.; Yang, Z. J.; Lodewijks, K.; Verre, R.; Shegai, T.; Andersson, P. O.; Käll, M. Dimer-on-Mirror

https://doi.org/10.1021/acsomega.3c08393
ACS Omega 2024, 9, 4819−4830

SERS Substrates with Attogram Sensitivity Fabricated by Colloidal Lithography. *Nanoscale* **2015**, *7* (21), 9405−9410.
(30) Rastogi, R.; Dogbe Foli, E. A.; Vincent, R.; Adam, P. M.; Krishnamoorthy, S. Engineering Electromagnetic Hot-Spots in Nanoparticle Cluster Arrays on Reflective Substrates for Highly Sensitive Detection of (Bio)Molecular Analytes. *ACS Appl. Mater. Interfaces* **2021**, *13* (28), 32653−32661.
(31) Dvoynenko, M. M.; Wang, H. H.; Hsiao, H. H.; Wang, Y. L.; Wang, J. K. Study of Signal-to-Background Ratio of Surface-Enhanced Raman Scattering: Dependences on Excitation Wavelength and Hot-Spot Gap. *J. Phys. Chem. C* **2017**, *121* (47), 26438−26445.
(32) Krishchenko, I.; Kravchenko, S.; Manoilov, E.; Korchovyi, A.; Snopok, B. Effect of Intense Hot-Spot-Specific Local Fields on Fluorescein Adsorbed at 3D Porous Gold Architecture: Evolution of SERS Amplification and Photobleaching under Resonant Illumination. *Eng. Proc.* **2023**, *35*, 32.
(33) Rahaman, M.; Milekhin, A. G.; Mukherjee, A.; Rodyakina, E. E.; Latyshev, A. V.; Dzhagan, V. M.; Zahn, D. R. T. The Role of a Plasmonic Substrate on the Enhancement and Spatial Resolution of Tip-Enhanced Raman Scattering. *Faraday Discuss.* **2019**, *214*, 309−323.
(34) Dan'ko, V.; Dmitruk, M.; Indutnyi, I.; Mamykin, S.; Myn'ko, V.; Shepeliavyi, P.; Lukaniuk, M.; Lytvyn, P. Au Gratings Fabricated by Interference Lithography for Experimental Study of Localized and Propagating Surface Plasmons. *Nanoscale Res. Lett.* **2017**, *12* (1), 190.
(35) Rahaman, M.; Moras, S.; He, L.; Madeira, T. I.; Zahn, D. R. T. Fine-Tuning of Localized Surface Plasmon Resonance of Metal Nanostructures from near-Infrared to Blue Prepared by Nanosphere Lithography. *J. Appl. Phys.* **2020**, *128* (23), No. 233104.
(36) Lim, H.; Kim, J.; Kani, K.; Masud, M. K.; Park, H.; Kim, M.; Alsheri, S. M.; Ahamad, T.; Alhokbany, N.; Na, J.; Malgras, V.; Bando, Y.; Yamauchi, Y. Designed Patterning of Mesoporous Metal Films Based on Electrochemical Micelle Assembly Combined with Lithographical Techniques. *Small* **2020**, *16* (12), No. 1902934.
(37) Lim, H.; Kim, D.; Kwon, G.; Kim, H. J.; You, J.; Kim, J.; Eguchi, M.; Nanjundan, A. K.; Na, J.; Yamauchi, Y. Synthesis of Uniformly Sized Mesoporous Silver Films and Their SERS Application. *J. Phys. Chem. C* **2020**, *124* (43), 23730−23737.
(38) Kim, D.; Kim, J.; Henzie, J.; Ko, Y.; Lim, H.; Kwon, G.; Na, J.; Kim, H. J.; Yamauchi, Y.; You, J. Mesoporous Au Films Assembled on Flexible Cellulose Nanopaper as High-Performance SERS Substrates. *Chem. Eng. J.* **2021**, *419*, No. 129445.
(39) Giordano, M. C.; Foti, A.; Messina, E.; Gucciardi, P. G.; Comoretto, D.; Buatier De Mongeot, F. SERS Amplification from Self-Organized Arrays of Plasmonic Nanocrescents. *ACS Appl. Mater. Interfaces* **2016**, *8* (10), 6629−6638.
(40) Tim, B.; Błaszkiewicz, P.; Kotkowiak, M. Recent Advances in Metallic Nanoparticle Assemblies for Surface-Enhanced Spectroscopy. *Int. J. Mol. Sci.* **2022**, *23*, 291.
(41) Mikac, L.; Ivanda, M.; Gotić, M.; Janicki, V.; Zorc, H.; Janči, T.; Vidaček, S. Surface-Enhanced Raman Spectroscopy Substrate Based on Ag-Coated Self-Assembled Polystyrene Spheres. *J. Mol. Struct.* **2017**, *1146*, 530−535.
(42) Smirnov, O.; Dzhagan, V.; Kovalenko, M.; Gudymenko, O.; Dzhagan, V.; Mazur, N.; Isaieva, O.; Maksimenko, Z.; Kondratenko, S.; Skoryk, M.; Yukhymchuk, V. ZnO and Ag NP-Decorated ZnO Nanoflowers: Green Synthesis Using Ganoderma Lucidum Aqueous Extract and Characterization. *RSC Adv.* **2022**, *13* (1), 756−763.
(43) Mikac, L.; Ivanda, M.; Đerek, V.; Gotić, M. Influence of Mesoporous Silicon Preparation Condition on Silver Clustering and SERS Enhancement. *J. Raman Spectrosc.* **2016**, *47* (9), 1036−1041.
(44) Mukherjee, A.; Wackenhut, F.; Dohare, A.; Horneber, A.; Lorenz, A.; Müchler, H.; Meixner, A. J.; Mayer, H. A.; Brecht, M. Three-Dimensional (3D) Surface-Enhanced Raman Spectroscopy (SERS) Substrates: Fabrication and SERS Applications. *J. Phys. Chem. C* **2023**, *127*, 13689−13698.
(45) Cai, W.; Wang, W.; Lu, L.; Chen, T. Coating Sulfonated Polystyrene Microspheres with Highly Dense Gold Nanoparticle Shell for SERS Application. *Colloid Polym. Sci.* **2013**, *291* (8), 2023−2029.
(46) Yukhymchuk, V. O.; Hreshchuk, O. M.; Dzhagan, V. M.; Matveevskaya, N. A.; Beynik, T. G.; Valakh, M. Y.; Sakhno, M. V.; Skoryk, M. A.; Lavoryk, S. R.; Rudko, G. Y.; Matveevskaya, N. A.; Beynik, T. G.; Valakh, M. Y. Experimental Studies and Modeling of " Starlike" Plasmonic Nanostructures for SERS Application. *Phys. Status Solidi B* **2019**, *256*, No. 1800280.
(47) Dzhagan, V. M.; Pirko, Ya. V.; Buziashvili, A. Yu.; Plokhovska, S. G.; Borova, M. M.; Yemets, A. I.; Mazur, N. V.; Kapush, O. A.; Yukhymchuk, V. O. Controlled Aggregation of Plasmonic Nanoparticles to Enhance the Efficiency of SERS Substrates. *Ukr. J. Phys.* **2022**, *67* (1), 80−87.
(48) Chen, L. M.; Liu, Y. N. Surface-Enhanced Raman Detection of Melamine on Silver-Nanoparticle- Decorated Silver/Carbon Nanospheres: Effect of Metal Ions. *ACS Appl. Mater. Interfaces* **2011**, *3* (8), 3091−3096.
(49) Schmit, V. L.; Martoglio, R.; Scott, B.; Strickland, A. D.; Carron, K. T. Lab-on-a-Bubble: Synthesis, Characterization, and Evaluation of Buoyant Gold Nanoparticle-Coated Silica Spheres. *J. Am. Chem. Soc.* **2012**, *134* (1), 59−62.
(50) Li, J. M.; Ma, W. F.; Wei, C.; You, L. J.; Guo, J.; Hu, J.; Wang, C. C. Detecting Trace Melamine in Solution by SERS Using Ag Nanoparticle Coated Poly(Styrene-Co-Acrylic Acid) Nanospheres as Novel Active Substrates. *Langmuir* **2011**, *27* (23), 14539−14544.
(51) Liu, T.; Li, D.; Yang, D.; Jiang, M. An Improved Seed-Mediated Growth Method to Coat Complete Silver Shells onto Silica Spheres for Surface-Enhanced Raman Scattering. *Colloids Surf., A* **2011**, *387* (1−3), 17−22.
(52) Li, J. M.; Ma, W. F.; Wei, C.; Guo, J.; Hu, J.; Wang, C. C. Poly(Styrene-Co-Acrylic Acid) Core and Silver Nanoparticle/Silica Shell Composite Microspheres as High Performance Surface-Enhanced Raman Spectroscopy (SERS) Substrate and Molecular Barcode Label. *J. Mater. Chem.* **2011**, *21* (16), 5992−5998.
(53) Zhu, W.; Wu, Y.; Yan, C.; Wang, C.; Zhang, M.; Wu, Z. Facile Synthesis of Mono-Dispersed Polystyrene (PS)/Ag Composite Microspheres via Modified Chemical Reduction. *Materials* **2013**, *6* (12), 5625−5638.
(54) Wang, W.; Ruan, C.; Gu, B. Development of Gold-Silica Composite Nanoparticle Substrates for Perchlorate Detection by Surface-Enhanced Raman Spectroscopy. *Anal. Chim. Acta* **2006**, *567* (1), 121−126.
(55) Fränzl, M.; Moras, S.; D Gordan, O.; R T Zahn, D. Interaction of One-Dimensional Photonic Crystals and Metal Nanoparticle Arrays and Its Application for Surface-Enhanced Raman Spectroscopy. *J. Phys. Chem. C* **2018**, *122* (18), 10153−10158.
(56) Dzhagan, V.; Smirnov, O.; Kovalenko, M.; Mazur, N.; Hreshchuk, O.; Taran, N.; Plokhovska, S.; Pirko, Y.; Yemets, A.; Yukhymchuk, V.; Zahn, D. R. T. Spectroscopic Study of Phytosynthesized Ag Nanoparticles and Their Activity as SERS Substrate. *Chemosensors* **2022**, *10*, 129.
(57) Borovaya, M.; Horiunova, I.; Plokhovska, S.; Pushkarova, N.; Blume, Y.; Yemets, A. Institute. Synthesis, Properties and Bioimaging Applications of Silver-Based Quantum Dots. *Int. J. Mol. Sci.* **2021**, *22*, 12202.
(58) Muntean, C. M.; Leopold, N.; Halmagyi, A.; Valimareanu, S. Surface-Enhanced Raman Scattering Assessment of DNA from Leaf Tissues Adsorbed on Silver Colloidal Nanoparticles. *J. Raman Spectrosc.* **2013**, *44*, 817−822.
(59) Krajczewski, J.; Joubert, V.; Kudelski, A. Light-Induced Transformation of Citrate-Stabilized Silver Nanoparticles: Photochemical Method of Increase of SERS Activity of Silver Colloids. *Colloids Surf., A* **2014**, *456*, 41−48.
(60) Mikac, L.; Kovačević, E.; Ukić, Š.; Raić, M.; Jurkin, T.; Marić, I.; Gotić, M.; Ivanda, M. Detection of Multi-Class Pesticide Residues with Surface-Enhanced Raman Spectroscopy. *Spectrochim. Acta, Part A* **2021**, *252*, No. 119478.
(61) Jaworska, A.; Wojcik, T.; Malek, K.; Kwolek, U.; Kepczynski, M.; Ansary, A. A.; Chlopicki, S.; Baranska, M. Rhodamine 6G Conjugated to Gold Nanoparticles as Labels for Both SERS and

https://doi.org/10.1021/acsomega.3c08393
ACS Omega 2024, 9, 4819−4830

Fluorescence Studies on Live Endothelial Cells. *Microchim. Acta* **2015**, *182*, 119−127.
(62) Strelchuk, V. V.; Kolomys, O. F.; Kaganovich, E. B.; Krishchenko, I. M.; Golichenko, B. O.; Boyko, M. I.; Kravchenko, S. O.; Kruglenko, I. V.; Lytvyn, O. S.; Manoilov, E. G.; Nasieka, I. M. Optical Characterization of SERS Substrates Based on Porous Au Films Prepared by Pulsed Laser Deposition. *J. Nanomater.* **2015**, *2015*, No. 203515.
(63) Krishchenko, I.; Kravchenko, S.; Kruglenko, I.; Manoilov, E.; Snopok, B. 3D Porous Plasmonic Nanoarchitectures for SERS-Based Chemical Sensing. *Eng. Proc.* **2022**, *27* (1), 41.
(64) Kim, D.; Lee, K.; Jeon, Y.; Kwon, G.; Kim, U. J.; Oh, C. S.; Kim, J.; You, J. Plasmonic Nanoparticle-Analyte Nanoarchitectronics Combined with Efficient Analyte Deposition Method on Regenerated Cellulose-Based SERS Platform. *Cellulose* **2021**, *28* (18), 11493−11502.
(65) Masud, M. K.; Na, J.; Lin, T. E.; Malgras, V.; Preet, A.; Ibn Sina, A. A.; Wood, K.; Billah, M.; Kim, J.; You, J.; Kani, K.; Whitten, A. E.; Salomon, C.; Nguyen, N. T.; Shiddiky, M. J. A.; Trau, M.; Hossain, M. S. A.; Yamauchi, Y. Nanostructured Mesoporous Gold Biosensor for MicroRNA Detection at Attomolar Level. *Biosens. Bioelectron.* **2020**, *168*, No. 112429.
(66) Song, S. W.; Kim, D.; Kim, J.; You, J.; Kim, H. M. Flexible Nanocellulose-Based SERS Substrates for Fast Analysis of Hazardous Materials by Spiral Scanning. *J. Hazard. Mater.* **2021**, *414*, No. 125160.
(67) Rastogi, R.; Arianfard, H.; Moss, D.; Juodkazis, S.; Adam, P. M.; Krishnamoorthy, S. Analyte Co-Localization at Electromagnetic Gap Hot-Spots for Highly Sensitive (Bio)Molecular Detection by Plasmon Enhanced Spectroscopies. *ACS Appl. Mater. Interfaces* **2021**, *13* (7), 9113−9121.
(68) Stöber, W.; Fink, A.; Ernst Bohn, D. Controlled Growth of Monodisperse Silica Spheres in the Micron Size Range. *J. Colloid Interface Sci.* **1968**, *26*, 62−69.
(69) Zhao, W.; Xiao, S.; Zhang, Y.; Pan, D.; Wen, J.; Qian, X.; Wang, D.; Cao, H.; He, W.; Quan, M.; Yang, Z. Binary "Island" Shaped Arrays with High-Density Hot Spots for Surface-Enhanced Raman Scattering Substrates. *Nanoscale* **2018**, *10* (29), 14220−14229.
(70) Jensen, R. A.; Sherin, J.; Emory, S. R. Single Nanoparticle Based Optical PH Probe. *Appl. Spectrosc.* **2007**, *61*, 832−838.
(71) Yukhymchuk, V.; Hreshchuk, O.; Valakh, My.; Skoryk, M.; Efanov, V.; Matveevskaya, N. Efficient Core-SiO_2/Shell-Au Nanostructures for Surface Enhanced Raman Scattering. *Semicond. Phys., Quantum Electron. Optoelectron.* **2014**, *17*, 217−221.
(72) Wu, J.; Chen, S.; Jia, W. Robust Phase Transfer, 3D-Assembly and SERS Application of Multi-Shaped Gold Nanoparticles. *J. Dispersion Sci. Technol.* **2021**, *42* (6), 824−834.
(73) Lupa, D.; Oćwieja, M.; Piergies, N.; Baliś, A.; Paluszkiewicz, C.; Adamczyk, Z. Gold Nanoparticles Deposited on Silica Microparticles - Electrokinetic Characteristics and Application in SERS. *Colloids Interface Sci. Commun.* **2019**, *33*, No. 100219.
(74) Yeshchenko, O. A.; Bondarchuk, I. S.; Malynych, S. Z.; Galabura, Y.; Chumanov, G.; Luzinov, I.; Pinchuk, A. O. Laser-Driven Hybridization of a Surface Plasmon Resonance Collective Mode in a Monolayer of Silver Nanoparticles. *Plasmonics* **2017**, *12* (5), 1571−1580.
(75) Dmitruk, I.; Blonskiy, I.; Pavlov, I.; Yeshchenko, O.; Alexeenko, A.; Dmytruk, A.; Korenyuk, P.; Kadan, V. Surface Plasmon as a Probe of Local Field Enhancement. *Plasmonics* **2009**, *4* (2), 115−119.
(76) Chegel, V.; Rachkov, O.; Lopatynskyi, A.; Ishihara, S.; Yanchuk, I.; Nemoto, Y.; Hill, J. P.; Ariga, K. Gold Nanoparticles Aggregation: Drastic Effect of Cooperative Functionalities in a Single Molecular Conjugate. *J. Phys. Chem. C* **2012**, *116*, 2683−2690.
(77) Cortijo-Campos, S.; Ramírez-Jiménez, R.; Climent-Pascual, E.; Aguilar-Pujol, M.; Jiménez-Villacorta, F.; Martínez, L.; Jiménez-Riobóo, R.; Prieto, C.; de Andrés, A. Raman Amplification in the Ultra-Small Limit of Ag Nanoparticles on SiO2 and Graphene: Size and Inter-Particle Distance Effects. *Mater. Des.* **2020**, *192*, No. 108702.
(78) Mukherjee, A.; Liu, Q.; Wackenhut, F.; Dai, F.; Fleischer, M.; Adam, P. M.; Meixner, A. J.; Brecht, M. Gradient SERS Substrates with Multiple Resonances for Analyte Screening: Fabrication and SERS Applications. *Molecules* **2022**, *27* (16), 5097.
(79) Wang, L.; Geng, Y.; Zhang, S.; Liang, J.; Xu, S.; Liu, Y. Propagating and Localized Surface Plasmon Co-Enhanced Raman Scattering Based on a Waveguide Coupling Surface Plasmon Resonance Structure. *J. Phys. Chem. C* **2023**, *127* (8), 4188−4194.
(80) Šimáková, P.; Kočišová, E.; Procházka, M. Coffee Ring" Effect of Ag Colloidal Nanoparticles Dried on Glass: Impact to Surface-Enhanced Raman Scattering (SERS). *J. Nanomater.* **2021**, *2021*, No. 4009352.
(81) Zhou, L.; Poggesi, S.; Bariani, G. C.; Mittapalli, R.; Adam, P. M.; Manzano, M.; Ionescu, R. E. Robust SERS Platforms Based on Annealed Gold Nanostructures Formed on Ultrafine Glass Substrates for Various (Bio)Applications. *Biosensors* **2019**, *9* (2), 53.
(82) Dvoynenko, M. M.; Kazantseva, Z. I.; Strelchuk, V. V.; Kolomys, O. F.; Bortshagovsky, E. G.; Venger, E. F.; Tronc, P. Probing Plasmonic System by the Simultaneous Measurement of Raman and Fluorescence Signals of Dye Molecules. *Semicond. Phys., Quantum Electron. Optoelectron.* **2011**, *14*, 195−199.
(83) Dvoynenko, M. M.; Kazantseva, Z. I.; Strelchuk, V. V.; Kolomys, O. F.; Venger, E. F.; Wang, J.-K. Molecular Ruler Based on Concurrent Measurements of Enhanced Raman Scattering and Fluorescence. *Opt. Lett.* **2010**, *35*, 3808−3810.
(84) Hou, X.; Wang, Q.; Mao, G.; Liu, H.; Yu, R.; Ren, X. Periodic Silver Nanocluster Arrays over Large-Area Silica Nanosphere Template as Highly Sensitive SERS Substrate. *Appl. Surf. Sci.* **2018**, *437*, 92−97.
(85) Chen, J.; Qin, G.; Shen, W.; Li, Y.; Das, B. Fabrication of Long-Range Ordered, Broccoli-like SERS Arrays and Application in Detecting Endocrine Disrupting Chemicals. *J. Mater. Chem. C* **2015**, *3* (6), 1309−1318.
(86) Ramuthai, M.; Habibuddin, S.; Sonia, S.; Jayram, N. D.; Deva Arun Kumar, K.; Shkir, M.; Algarni, H.; AlFaify, S. Surface-Enhanced Raman Spectroscopy Studies of Orderly Arranged Silica Nanospheres-Synthesis, Characterization and Dye Detection. *J. Mater. Sci.: Mater. Electron.* **2021**, *32* (22), 26596−26607.

https://doi.org/10.1021/acsomega.3c08393
ACS Omega 2024, 9, 4819−4830